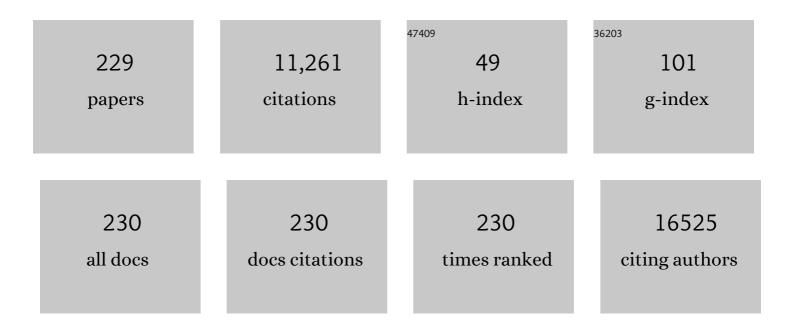
List of Publications by Year in descending order

Source: https://exaly.com/author-pdf/7386972/publications.pdf Version: 2024-02-01



WOLFCANC HELŸ

#	Article	IF	CITATIONS
1	Highly Stable Lasing from Solutionâ€Epitaxially Grown Formamidiniumâ€Leadâ€Bromide Microâ€Resonators. Advanced Optical Materials, 2022, 10, .	3.6	3
2	Selfâ€Healing Cs ₃ Bi ₂ Br ₃ I ₆ Perovskite Wafers for Xâ€Ray Detection. Advanced Functional Materials, 2021, 31, 2102713.	7.8	29
3	High-sensitivity high-resolution X-ray imaging with soft-sintered metal halide perovskites. Nature Electronics, 2021, 4, 681-688.	13.1	149
4	The Fine-Structure Constant as a Ruler for the Band-Edge Light Absorption Strength of Bulk and Quantum-Confined Semiconductors. Nano Letters, 2021, 21, 9426-9432.	4.5	1
5	Perspectives of solution epitaxially grown defect tolerant lead-halide-perovskites and lead-chalcogenides. Applied Physics Letters, 2021, 119, .	1.5	2
6	Exfoliated CrPS 4 with Promising Photoconductivity. Small, 2020, 16, 1905924.	5.2	26
7	Graphene Oxide Thin Films: Synthesis and Optical Characterization. ChemistrySelect, 2020, 5, 11737-11744.	0.7	15
8	Epitaxial Metal Halide Perovskites by Inkjetâ€Printing on Various Substrates. Advanced Functional Materials, 2020, 30, 2004612.	7.8	21
9	Micron Thick Colloidal Quantum Dot Solids. Nano Letters, 2020, 20, 5284-5291.	4.5	47
10	Sensitive Direct Converting Xâ€Ray Detectors Utilizing Crystalline CsPbBr ₃ Perovskite Films Fabricated via Scalable Melt Processing. Advanced Materials Interfaces, 2020, 7, 1901575.	1.9	83
11	Effect of Ligand Treatment on the Tuning of Infrared Plasmonic Indium Tin Oxide Nanocrystal Electrochromic Devices. Advanced Engineering Materials, 2020, 22, 2000112.	1.6	15
12	Looking beyond the Surface: The Band Gap of Bulk Methylammonium Lead Iodide. Nano Letters, 2020, 20, 3090-3097.	4.5	16
13	A perspective on the bright future of metal halide perovskites for X-ray detection. Applied Physics Letters, 2019, 115, .	1.5	45
14	Fully Printed Infrared Photodetectors from PbS Nanocrystals with Perovskite Ligands. ACS Nano, 2019, 13, 2389-2397.	7.3	30
15	Pushing PbS/Metalâ€Halideâ€Perovskite Core/Epitaxialâ€Ligandâ€Shell Nanocrystal Photodetectors beyond 3 µm Wavelength. Advanced Functional Materials, 2019, 29, 1807964.	7.8	35
16	Photophysical and electronic properties of bismuth-perovskite shelled lead sulfide quantum dots. Journal of Chemical Physics, 2019, 151, 214702.	1.2	1
17	Interplay between crystal structure, shape and functionality of colloidal nanocrystals and supercrystals. Acta Crystallographica Section A: Foundations and Advances, 2019, 75, e657-e657.	0.0	0
18	General Observation of Photocatalytic Oxygen Reduction to Hydrogen Peroxide by Organic Semiconductor Thin Films and Colloidal Crystals. ACS Applied Materials & Interfaces, 2018, 10, 13253-13257.	4.0	37

#	Article	IF	CITATIONS
19	Revealing Trap States in Lead Sulphide Colloidal Quantum Dots by Photoinduced Absorption Spectroscopy. Advanced Electronic Materials, 2018, 4, 1700348.	2.6	25
20	A Shapeâ€Induced Orientation Phase within 3D Nanocrystal Solids. Advanced Materials, 2018, 30, e1802078.	11.1	7
21	Broadening of Distribution of Trap States in PbS Quantum Dot Field-Effect Transistors with High- <i>k</i> Dielectrics. ACS Applied Materials & Interfaces, 2017, 9, 4719-4724.	4.0	20
22	Quasi-epitaxial Metal-Halide Perovskite Ligand Shells on PbS Nanocrystals. ACS Nano, 2017, 11, 1246-1256.	7.3	74
23	Enabling Ambipolar to Heavy n-Type Transport in PbS Quantum Dot Solids through Doping with Organic Molecules. ACS Applied Materials & Interfaces, 2017, 9, 18039-18045.	4.0	34
24	High-performance direct conversion X-ray detectors based on sintered hybrid lead triiodide perovskite wafers. Nature Photonics, 2017, 11, 436-440.	15.6	442
25	Strainâ€Modulated Charge Transport in Flexible PbS Nanocrystal Fieldâ€Effect Transistors. Advanced Electronic Materials, 2017, 3, 1600360.	2.6	20
26	Cellular interfaces with hydrogen-bonded organic semiconductor hierarchical nanocrystals. Nature Communications, 2017, 8, 91.	5.8	51
27	Morphology-Controlled Organic Solar Cells Improved by a Nanohybrid System of Single Wall Carbon Nanotubes Sensitized by PbS Core/Perovskite Epitaxial Ligand Shell Quantum Dots. Solar Rrl, 2017, 1, 1700043.	3.1	7
28	Carbon Photodetectors: The Versatility of Carbon Allotropes. Advanced Energy Materials, 2017, 7, 1601574.	10.2	44
29	Hydrogenâ€Bonded Organic Semiconductors as Stable Photoelectrocatalysts for Efficient Hydrogen Peroxide Photosynthesis. Advanced Functional Materials, 2016, 26, 5248-5254.	7.8	115
30	Tunable doping in PbS nanocrystal field-effect transistors using surface molecular dipoles. APL Materials, 2016, 4, 116105.	2.2	10
31	Perovskites target X-ray detection. Nature Photonics, 2016, 10, 288-289.	15.6	112
32	Photocatalysis: Hydrogen-Bonded Organic Semiconductors as Stable Photoelectrocatalysts for Efficient Hydrogen Peroxide Photosynthesis (Adv. Funct. Mater. 29/2016). Advanced Functional Materials, 2016, 26, 5247-5247.	7.8	1
33	Galvanic Exchange in Colloidal Metal/Metal-Oxide Core/Shell Nanocrystals. Journal of Physical Chemistry C, 2016, 120, 19848-19855.	1.5	9
34	Detection of X-ray photons by solution-processed lead halide perovskites. Nature Photonics, 2015, 9, 444-449.	15.6	916
35	lodideâ€Capped PbS Quantum Dots: Full Optical Characterization of a Versatile Absorber. Advanced Materials, 2015, 27, 1533-1539.	11.1	14
36	Prospects of Nanoscience with Nanocrystals. ACS Nano, 2015, 9, 1012-1057.	7.3	1,005

#	Article	IF	CITATIONS
37	High Mobility and Low Density of Trap States in Dualâ€Solidâ€Gated PbS Nanocrystal Fieldâ€Effect Transistors. Advanced Materials, 2015, 27, 2107-2112.	11.1	55
38	Enhanced near-infrared response of nano- and microstructured silicon/organic hybrid photodetectors. Applied Physics Letters, 2015, 107, .	1.5	16
39	Low-threshold amplified spontaneous emission and lasing from colloidal nanocrystals of caesium lead halide perovskites. Nature Communications, 2015, 6, 8056.	5.8	1,278
40	Random Lasing with Systematic Threshold Behavior in Films of CdSe/CdS Core/Thick-Shell Colloidal Quantum Dots. ACS Nano, 2015, 9, 9792-9801.	7.3	49
41	Charge transport in nanoparticular thin films of zinc oxide and aluminum-doped zinc oxide. Journal of Materials Chemistry C, 2015, 3, 1468-1472.	2.7	10
42	High Infrared Photoconductivity in Films of Arsenic-Sulfide-Encapsulated Lead-Sulfide Nanocrystals. ACS Nano, 2014, 8, 12883-12894.	7.3	62
43	Crystal Phase Transitions in the Shell of PbS/CdS Core/Shell Nanocrystals Influences Photoluminescence Intensity. Chemistry of Materials, 2014, 26, 5914-5922.	3.2	44
44	Reducing charge trapping in PbS colloidal quantum dot solids. Applied Physics Letters, 2014, 104, .	1.5	65
45	The potential of Rutherford Backscattering Spectrometry for composition analysis of colloidal nanocrystals. Nuclear Instruments & Methods in Physics Research B, 2014, 332, 122-125.	0.6	2
46	Tuning the Localized Surface Plasmon Resonance in Cu _{2–<i>x</i>} Se Nanocrystals by Postsynthetic Ligand Exchange. ACS Applied Materials & Interfaces, 2014, 6, 17770-17775.	4.0	68
47	Polarization control of metal-enhanced fluorescence in hybrid assemblies of photosynthetic complexes and gold nanorods. Physical Chemistry Chemical Physics, 2014, 16, 9015.	1.3	15
48	Hydrogen-Bonded Organic Semiconductor Micro- And Nanocrystals: From Colloidal Syntheses to (Opto-)Electronic Devices. Journal of the American Chemical Society, 2014, 136, 16522-16532.	6.6	75
49	Determination of the Electronic Energy Levels of Colloidal Nanocrystals using Fieldâ€Effect Transistors and Abâ€Initio Calculations. Advanced Materials, 2014, 26, 5639-5645.	11.1	33
50	Structural Profiles of Nanocrystals from ASAXS and Crystallographic Techniques. Acta Crystallographica Section A: Foundations and Advances, 2014, 70, C1583-C1583.	0.0	0
51	Photovoltaic properties of thin film heterojunctions with cupric oxide absorber. Journal of Renewable and Sustainable Energy, 2013, 5, .	0.8	58
52	Highly Luminescent, Size- and Shape-Tunable Copper Indium Selenide Based Colloidal Nanocrystals. Chemistry of Materials, 2013, 25, 3753-3757.	3.2	113
53	Sizeâ€Đependent Charge Transfer in Blends of PbS Quantum Dots with a Lowâ€Gap Siliconâ€Bridged Copolymer. Advanced Energy Materials, 2013, 3, 1490-1499.	10.2	29
54	Concentration and excitation effects on the exciton dynamics of poly(3-hexylthiophene)/PbS quantum dot blend films. Nanotechnology, 2013, 24, 235707.	1.3	4

#	Article	IF	CITATIONS
55	Tuning the Magnetic Properties of Metal Oxide Nanocrystal Heterostructures by Cation Exchange. Nano Letters, 2013, 13, 586-593.	4.5	91
56	Low Driving Voltage and High Mobility Ambipolar Fieldâ€Effect Transistors with PbS Colloidal Nanocrystals. Advanced Materials, 2013, 25, 4309-4314.	11.1	107
57	Short-wave infrared colloidal quantum dot photodetectors on silicon. Proceedings of SPIE, 2013, , .	0.8	7
58	Charge separation dynamics in a narrow band gap polymer–PbS nanocrystal blend for efficient hybrid solar cells. Journal of Materials Chemistry, 2012, 22, 24411.	6.7	48
59	Plasmon-enhanced fluorescence in heterochlorophyllous peridinin-chlorophyll-protein photosynthetic complex. Optical Materials, 2012, 34, 2076-2079.	1.7	6
60	Carbon nanotube growth from Langmuir–Blodgett deposited Fe3O4nanocrystals. Nanotechnology, 2012, 23, 405604.	1.3	6
61	High precision positioning of plasmonic nanoparticle based on damascene process. , 2012, , .		0
62	From Highly Monodisperse Indium and Indium Tin Colloidal Nanocrystals to Self-Assembled Indium Tin Oxide Nanoelectrodes. ACS Nano, 2012, 6, 4113-4121.	7.3	48
63	Exploring the Origin of the Temperatureâ€Dependent Behavior of PbS Nanocrystal Thin Films and Solar Cells. Advanced Functional Materials, 2012, 22, 1598-1605.	7.8	71
64	Spectral Dependence of Fluorescence Enhancement in LH2-Au Nanoparticle Hybrid Nanostructures. Acta Physica Polonica A, 2012, 122, 252-254.	0.2	4
65	Fluorescence Mapping of PCP Light-Harvesting Complexes Coupled to Silver Nanowires. Acta Physica Polonica A, 2012, 122, 259-262.	0.2	3
66	Fluorescence Microscopy of Corrole-Single Silver Nanowire Hybrid Nanostructures. Acta Physica Polonica A, 2012, 122, 333-336.	0.2	2
67	Evaluation of Ordering in Single-Component and Binary Nanocrystal Superlattices by Analysis of Their Autocorrelation Functions. ACS Nano, 2011, 5, 1703-1712.	7.3	30
68	Infrared Emitting and Photoconducting Colloidal Silver Chalcogenide Nanocrystal Quantum Dots from a Silylamide-Promoted Synthesis. ACS Nano, 2011, 5, 3758-3765.	7.3	164
69	Substantial Temperature Dependence of Transverse Electron gâ^—-factor in Lead Chalcogenide Multi-quantum Wells. AIP Conference Proceedings, 2011, , .	0.3	0
70	Quasistatic Dielectric Constants Of Colloidal Nanocrystals. , 2011, , .		0
71	Temperature dependent photoresponse from colloidal PbS quantum dot sensitized inorganic/organic hybrid photodiodes. Applied Physics Letters, 2011, 98, .	1.5	18
72	Mapping the Local Photoresponse of Epitaxial and Colloidal Quantum Dots by Photoconductive Atomic Force Microscopy. , 2011, , .		0

#	Article	IF	CITATIONS
73	AFMâ€based photocurrent imaging of epitaxial and colloidal QDs. Physica Status Solidi C: Current Topics in Solid State Physics, 2011, 8, 426-428.	0.8	1
74	Charge‧eparation Dynamics in Inorganic–Organic Ternary Blends for Efficient Infrared Photodiodes. Advanced Functional Materials, 2011, 21, 1988-1992.	7.8	61
75	Optical Properties of Organic Semiconductor Blends with Nearâ€Infrared Quantumâ€Dot Sensitizers for Light Harvesting Applications. Advanced Energy Materials, 2011, 1, 802-812.	10.2	88
76	Growth and characterization of mid-infrared microdisk lasers operating in continuous-wave mode up to 2°C. Journal of Crystal Growth, 2011, 323, 460-462.	0.7	3
77	Fluorescence enhancement of light-harvesting complex 2 from purple bacteria coupled to spherical gold nanoparticles. Applied Physics Letters, 2011, 99, .	1.5	46
78	Midinfrared electroluminescence from PbTe/CdTe quantum dot light-emitting diodes. Applied Physics Letters, 2011, 98, .	1.5	36
79	Scanning microwave microscopy and scanning capacitance microscopy on colloidal nanocrystals. Journal of Applied Physics, 2011, 109, 064313.	1.1	9
80	Variable wavelength photocurrent mapping on PbS quantum dot: fullerene thin films by conductive atomic force microscopy. Semiconductor Science and Technology, 2011, 26, 095002.	1.0	3
81	Size-Dependent Electron Transfer from Colloidal PbS Nanocrystals to Fullerene. Journal of Physical Chemistry Letters, 2010, 1, 1149-1154.	2.1	54
82	Damascene Process for Controlled Positioning of Magnetic Colloidal Nanocrystals. Advanced Materials, 2010, 22, 1364-1368.	11.1	8
83	Publisher's Note: Magnetic polarons in Eu-based films of magnetic semiconductors [Phys. Rev. B 81 , 153201 (2010)]. Physical Review B, 2010, 81, .	1.1	0
84	Enhanced color conversion from colloidal CdSe/CdS dot/rods by vertical microcavities. Applied Physics Letters, 2010, 97, 111115.	1.5	7
85	Magnetic polarons in Eu-based films of magnetic semiconductors. Physical Review B, 2010, 81, .	1.1	24
86	Energetic and Entropic Contributions to Self-Assembly of Binary Nanocrystal Superlattices: Temperature as the Structure-Directing Factor. Journal of the American Chemical Society, 2010, 132, 11967-11977.	6.6	210
87	PbS nanocrystal solar cells with high efficiency and fill factor. Applied Physics Letters, 2010, 97, .	1.5	108
88	Large-Area Ordered Superlattices from Magnetic Wüstite/Cobalt Ferrite Core/Shell Nanocrystals by Doctor Blade Casting. ACS Nano, 2010, 4, 423-431.	7.3	83
89	Near room temperature continuous-wave laser operation from type-I interband transitions at wavelengths beyond 4â€,î¼m. Applied Physics Letters, 2010, 97, 061103.	1.5	26
90	Highly Monodisperse Bismuth Nanoparticles and Their Three-Dimensional Superlattices. Journal of the American Chemical Society, 2010, 132, 15158-15159.	6.6	91

#	Article	IF	CITATIONS
91	Langmuirâ~'Schaefer Deposition of Quantum Dot Multilayers. Langmuir, 2010, 26, 7732-7736.	1.6	54
92	Exchange interactions in europium monochalcogenide magnetic semiconductors and their dependence on hydrostatic strain. Physical Review B, 2010, 81, .	1.1	47
93	Surface modification of semiconductor nanocrystals by a methanofullerene carboxylic acid. Journal of Materials Chemistry, 2010, 20, 8470.	6.7	11
94	Lead salt microdisk lasers operating in continuous wave mode at 5.3â€,μm wavelength. Applied Physics Letters, 2009, 94, 021118.	1.5	17
95	Enhanced infrared emission from colloidal HgTe nanocrystal quantum dots on silicon-on-insulator photonic crystals. Applied Physics Letters, 2009, 95, 053107.	1.5	7
96	Coherent {001} interfaces between rocksalt and zinc-blende crystal structures. Physical Review B, 2009, 79, .	1.1	21
97	Para-sexiphenyl-CdSe/ZnS nanocrystal hybrid light emitting diodes. Applied Physics Letters, 2009, 94, .	1.5	19
98	PbTe and SnTe quantum dot precipitates in a CdTe matrix fabricated by ion implantation. Journal of Applied Physics, 2009, 106, .	1.1	8
99	Para-sexiphenyl-CdSe Nanocrystals Hybrid Light Emitting Diodes with Optimized Layer Thickness and Interfaces. Materials Research Society Symposia Proceedings, 2009, 1154, 1.	0.1	0
100	Solutionâ€Processable Nearâ€IR Photodetectors Based on Electron Transfer from PbS Nanocrystals to Fullerene Derivatives. Advanced Materials, 2009, 21, 683-687.	11.1	121
101	Exciton–Exciton Interaction and Optical Gain in Colloidal CdSe/CdS Dot/Rod Nanocrystals. Advanced Materials, 2009, 21, 4942-4946.	11.1	82
102	Exchange oupled Bimagnetic Wüstite/Metal Ferrite Core/Shell Nanocrystals: Size, Shape, and Compositional Control. Small, 2009, 5, 2247-2252.	5.2	78
103	Near-infrared imaging with quantum-dot-sensitized organic photodiodes. Nature Photonics, 2009, 3, 332-336.	15.6	598
104	Quasiâ€Seeded Growth of Ligandâ€Tailored PbSe Nanocrystals through Cationâ€Exchangeâ€Mediated Nucleation. Angewandte Chemie - International Edition, 2008, 47, 3029-3033.	7.2	103
105	Gold/Iron Oxide Core/Hollow‧hell Nanoparticles. Advanced Materials, 2008, 20, 4323-4329.	11.1	308
106	Highly efficient (infra)red conversion of InGaN light emitting diodes by nanocrystals, enhanced by colour selective mirrors. Nanotechnology, 2008, 19, 355205.	1.3	2
107	Size-controlled quantum dots fabricated by precipitation of epitaxially grown, immiscible semiconductor heterosystems. Journal of Physics Condensed Matter, 2008, 20, 454216.	0.7	4
108	Temperature-dependent midinfrared photoluminescence of epitaxial PbTe/CdTe quantum dots and calculation of the corresponding transition energy. Physical Review B, 2008, 78, .	1.1	50

#	Article	IF	CITATIONS
109	Energy transfer in close-packed PbS nanocrystal films. Physical Review B, 2008, 77, .	1.1	49
110	Tuning spin properties of excitons in single CdTe quantum dots by annealing. Nanotechnology, 2008, 19, 125706.	1.3	5
111	Antiferromagnetic Order with Atomic Layer Resolution In EuTe(111) Films. Physical Review Letters, 2008, 101, 267202.	2.9	19
112	Quantum dot nanocolumn photodetectors for light detection in the infrared. Applied Physics Letters, 2008, 92, 261113.	1.5	15
113	Preparation of catalytic nano-particles and growth of aligned CNTs with HF-CVD. Journal of Physics: Conference Series, 2008, 100, 052092.	0.3	1
114	Highly efficient (infra)-red-conversion of InGaN light emitting diodes by nanocrystals, enhanced by color selective mirrors. Proceedings of SPIE, 2008, , .	0.8	0
115	Mid-infrared vertical-cavity surface-emitting lasers based on lead salt/BaF 2 Bragg mirrors. Proceedings of SPIE, 2008, , .	0.8	0
116	Monte Carlo Simulation of Electron Transport in PbTe. Springer Proceedings in Physics, 2008, , 77-79.	0.1	0
117	Size control and midinfrared emission of epitaxial PbTeâ^CdTe quantum dot precipitates grown by molecular beam epitaxy. Applied Physics Letters, 2007, 91, 222106.	1.5	57
118	Quantum dots with coherent interfaces between rocksalt-PbTe and zincblende-CdTe. Journal of Applied Physics, 2007, 101, 081723.	1.1	28
119	Mid-infrared high finesse microcavities and vertical-cavity lasers based on IV–VI semiconductor/BaF2 broadband Bragg mirrors. Journal of Applied Physics, 2007, 101, 093102.	1.1	17
120	Fatty Acid Salts as Stabilizers in Size- and Shape-Controlled Nanocrystal Synthesis:  The Case of Inverse Spinel Iron Oxide. Journal of the American Chemical Society, 2007, 129, 6352-6353.	6.6	380
121	SnTe Nanocrystals:  A New Example of Narrow-Gap Semiconductor Quantum Dots. Journal of the American Chemical Society, 2007, 129, 11354-11355.	6.6	156
122	Emission Properties of 6.7 Micron Vertical-Emitting Microcavity Lasers Operating in Continuous-Wave Mode. AIP Conference Proceedings, 2007, , .	0.3	0
123	Inkjetâ€Printed Nanocrystal Photodetectors Operating up to 3 μm Wavelengths. Advanced Materials, 2007 19, 3574-3578.	' 11.1	180
124	Structural and electronic properties of PbTe (rocksalt)/CdTe (zinc-blende) interfaces. Applied Surface Science, 2007, 254, 397-400.	3.1	7
125	The coherent {100} and {110} interfaces between rocksalt-PbTe and zincblende-CdTe. Journal of Crystal Growth, 2007, 301-302, 671-675.	0.7	4
126	Photoluminescence characterization of PbTe/CdTe quantum dots grown by lattice-type mismatched epitaxy. Journal of Crystal Growth, 2007, 301-302, 722-725.	0.7	28

#	Article	IF	CITATIONS
127	Quantum confinement in layer-by-layer deposited colloidal HgTe nanocrystals determined by spectroscopic ellipsometry. Applied Surface Science, 2007, 254, 291-294.	3.1	10
128	Colloidal HgTe Nanocrystals with Widely Tunable Narrow Band Gap Energies:Â From Telecommunications to Molecular Vibrations. Journal of the American Chemical Society, 2006, 128, 3516-3517.	6.6	176
129	Rebonding at coherent interfaces between rocksalt-PbTe/zinc-blende-CdTe. New Journal of Physics, 2006, 8, 317-317.	1.2	32
130	Spectroscopic ellipsometry of layer by layer deposited colloidal HgTe nanocrystals exhibiting quantum confinement. Physica E: Low-Dimensional Systems and Nanostructures, 2006, 32, 104-107.	1.3	9
131	Highly luminescent nanocrystal quantum dots fabricated by lattice-type mismatched epitaxy. Physica E: Low-Dimensional Systems and Nanostructures, 2006, 35, 241-245.	1.3	8
132	On inverse systems and squarefree decomposition of zero-dimensional polynomial ideals. Journal of Symbolic Computation, 2006, 41, 261-284.	0.5	3
133	Hybrid Solar Cells Using HgTe Nanocrystals and Nanoporous TiO2 Electrodes. Advanced Functional Materials, 2006, 16, 1095-1099.	7.8	69
134	Centrosymmetric PbTeâ^•CdTe quantum dots coherently embedded by epitaxial precipitation. Applied Physics Letters, 2006, 88, 192109.	1.5	95
135	Room temperature operation of epitaxial lead-telluride detectors monolithically integrated on midinfrared filters. Applied Physics Letters, 2006, 88, 041105.	1.5	29
136	Effect of quantum confinement on higher transitions in HgTe nanocrystals. Applied Physics Letters, 2006, 89, 193114.	1.5	20
137	Highly efficient epitaxial Bragg mirrors with broad omnidirectional reflectance bands in the midinfrared. Applied Physics Letters, 2006, 89, 051110.	1.5	13
138	Two- and one-dimensional light propagations and gain in layer-by-layer-deposited colloidal nanocrystal waveguides. Applied Physics Letters, 2006, 89, 111120.	1.5	12
139	Mid-infrared Vertical Cavity Surface Emitting Lasers based on the Lead Salt Compounds. Springer Series in Optical Sciences, 2006, , 265-301.	0.5	8
140	Molecular beam epitaxy of vertical-emitting microcavity lasers for the 6–8micron spectral range operating in continuous-wave mode. Journal of Crystal Growth, 2005, 278, 723-727.	0.7	0
141	Nanocrystal-based microcavity light-emitting devices operating in the telecommunication wavelength range. Applied Physics Letters, 2005, 86, 241104.	1.5	16
142	Magnetic field tunable circularly polarized stimulated emission from midinfrared IV-VI vertical emitting lasers. Applied Physics Letters, 2005, 86, 021109.	1.5	5
143	Emission properties of 6.7μm continuous-wave PbSe-based vertical-emitting microcavity lasers operating up to 100K. Applied Physics Letters, 2005, 86, 031102.	1.5	30
144	Sensitivity of exciton spin relaxation in quantum dots to confining potential. Applied Physics Letters, 2005, 86, 103101.	1.5	17

#	ARTICLE	IF	CITATIONS
145	Negatively charged excitons as an optical probe of spin injection from Cd0.73Mg0.24Mn0.03Te spin aligner into a graded bandgap Cd1AxMgxTe/CdTe quantum well structure. Semiconductor Science and Technology, 2004, 19, 359-365.	1.0	3
146	IV–VI resonant-cavity enhanced photodetectors for the mid-infrared. Semiconductor Science and Technology, 2004, 19, L115-L117.	1.0	16
147	Impact of carrier redistribution on the photoluminescence of CdTe self-assembled quantum dot ensembles. Physical Review B, 2004, 69, .	1.1	37
148	Resonant spectroscopy of II-VI self-assembled quantum dots: Excited states and exciton–longitudinal optical phonon coupling. Physical Review B, 2004, 70, .	1.1	30
149	Magnetic polaron induced near-band-gap luminescence in epitaxial EuTe. Physical Review B, 2004, 70, .	1.1	24
150	Hysteresis loops of the energy band gap and effective g factor up to 18 000 for metamagnetic EuSe epilayers. Applied Physics Letters, 2004, 85, 67-69.	1.5	9
151	Highly directional emission from colloidally synthesized nanocrystals in vertical cavities with small mode spacing. Applied Physics Letters, 2004, 84, 2223-2225.	1.5	16
152	Tuning the optical and magnetic properties of Il–VI quantum dots by post-growth rapid thermal annealing. Physica Status Solidi (B): Basic Research, 2004, 241, 652-655.	0.7	5
153	Exciton-LO phonon interaction in II-VI self-assembled quantum dots. Physica Status Solidi C: Current Topics in Solid State Physics, 2004, 1, 767-770.	0.8	5
154	Continuous-wave emission from midinfrared IV–VI vertical-cavity surface-emitting lasers. Applied Physics Letters, 2004, 84, 3268-3270.	1.5	19
155	Optical studies of zero-field magnetization of CdMnTe quantum dots: Influence of average size and composition of quantum dots. Journal of Applied Physics, 2004, 96, 7407-7413.	1.1	16
156	Vertical-cavity surface-emitting lasers in the 8-/spl mu/m midinfrared spectral range with continuous-wave and pulsed emission. IEEE Journal of Quantum Electronics, 2004, 40, 966-969.	1.0	7
157	Molecular Beam Epitaxial Growth and Photoluminescence Characterization of PbTe/CdTe Quantum Wells for Mid-Infrared Optical Devices. Zairyo/Journal of the Society of Materials Science, Japan, 2004, 53, 1328-1333.	0.1	0
158	Anomalous Magneto-Optical Properties of EuTe Induced by Magnetic Polarons. Journal of Superconductivity and Novel Magnetism, 2003, 16, 403-405.	0.5	2
159	Applications of lead-salt microcavities for mid-infrared devices. IEE Proceedings: Optoelectronics, 2003, 150, 332.	0.8	15
160	Optical properties of annealed CdTe self-assembled quantum dots. Applied Physics Letters, 2003, 83, 254-256.	1.5	27
161	Tuning the properties of magnetic CdMnTe quantum dots. Applied Physics Letters, 2003, 83, 3575-3577.	1.5	37
162	Spin injection through different g-factor heterointerfaces using negative trions for spin detection. Applied Physics Letters, 2003, 82, 541-543.	1.5	11

#	Article	IF	CITATIONS
163	Midinfrared continuous-wave photoluminescence of lead–salt structures up to temperatures of 190 °C. Applied Physics Letters, 2003, 82, 4065-4067.	1.5	44
164	Magnetization and spin distribution of single sub-monolayers of MnTe in semiconductor quantum wells. Physical Review B, 2003, 68, .	1.1	5
165	Midinfrared IV–VI vertical-cavity surface-emitting lasers with zero-, two-, and three-dimensional systems in the active regions. Applied Physics Letters, 2002, 81, 208-210.	1.5	43
166	Correlation between exciton decay time and Stokes shift in digital magnetic heterostructures. Physical Review B, 2002, 65, .	1.1	6
167	Midinfrared absorption ofPbSe/Pb1â^'xEuxTequantum dot superlattices in IV-VI microcavities. Physical Review B, 2002, 65, .	1.1	11
168	Colloidally synthesised semiconductor nanocrystals in resonant cavity light emitting devices. Electronics Letters, 2002, 38, 1373.	0.5	2
169	Growth and Optical Properties of Mn-Containing II-VI Quantum Dots. Physica Status Solidi (B): Basic Research, 2002, 229, 469-472.	0.7	29
170	Optical properties of CdTe/ZnTe quantum dot superlattices. Physica E: Low-Dimensional Systems and Nanostructures, 2002, 12, 503-506.	1.3	9
171	Fabrication of 3.9– mid-infrared surface emitting PbSe/PbEuTe quantum dot lasers using molecular beam epitaxy. Physica E: Low-Dimensional Systems and Nanostructures, 2002, 13, 876-880.	1.3	8
172	Above-room-temperature operation of IV–VI microcavity lasers. Physica E: Low-Dimensional Systems and Nanostructures, 2002, 13, 888-891.	1.3	0
173	Er3+- emission from organic complexes embedded in thin polymer films. Synthetic Metals, 2001, 121, 1511-1512.	2.1	12
174	Lead-salt-based VCSELs for the 3- to 6-î¼m range. , 2001, , .		0
175	Epitaxial Bragg mirrors for the mid-infrared and their applications. Progress in Quantum Electronics, 2001, 25, 193-228.	3.5	53
176	Giant tunability of excitonic photoluminescence transitions in antiferromagnetic EuTe epilayers induced by magnetic polarons. Physica E: Low-Dimensional Systems and Nanostructures, 2001, 10, 419-423.	1.3	2
177	Optical Characterization of Self-Organized PbSe/Pb1-xEuxTe Quantum Dot Superlattices. Physica Status Solidi (B): Basic Research, 2001, 224, 223-227.	0.7	3
178	Thermal Carrier Escape and Capture in CdTe Quantum Dots. Physica Status Solidi (B): Basic Research, 2001, 224, 465-469.	0.7	11
179	Spectroscopy on Vertical Microcavities for the Mid-Infrared. Physica Status Solidi A, 2001, 188, 929-935.	1.7	2
180	Molecular beam epitaxy of lead salt-based vertical cavity surface emitting lasers for the 4–6μm spectral region. Journal of Crystal Growth, 2001, 227-228, 722-728.	0.7	2

#	Article	IF	CITATIONS
181	Magnetic-field-tunable photoluminescence transitions in antiferromagnetic EuTe epilayers layers with an effective g factor of 1140. Applied Physics Letters, 2001, 78, 3484-3486.	1.5	18
182	Midinfrared surface-emitting PbSe/PbEuTe quantum-dot lasers. Applied Physics Letters, 2001, 79, 1225-1227.	1.5	70
183	Structural and optical evidence of island correlation in CdTe/ZnTe superlattices. Applied Physics Letters, 2001, 78, 3884-3886.	1.5	42
184	Semimagnetic self-organized Cd1â^'xMnxTe quantum dots generated by postgrowth thermal annealing. Applied Physics Letters, 2001, 78, 2140-2142.	1.5	15
185	Above-room-temperature mid-infrared lasing from vertical-cavity surface-emitting PbTe quantum-well lasers. Applied Physics Letters, 2001, 78, 862-864.	1.5	55
186	Giant tunability of exciton photoluminescence emission in antiferromagnetic EuTe. Physical Review B, 2001, 63, .	1.1	27
187	Strongly detuned IV-VI microcavity and microdisk resonances: mode splitting and lasing. Springer Proceedings in Physics, 2001, , 677-678.	0.1	0
188	Zeeman mapping of probability densities in square quantum wells using ultranarrow probes. Springer Proceedings in Physics, 2001, , 467-468.	0.1	0
189	Giant tunability of excitonic photoluminescence transitions in antiferromagnetic EuTe epilayers. Springer Proceedings in Physics, 2001, , 240-241.	0.1	0
190	Magnetization of single MnTe (sub)monolayers embedded in nonmagnetic quantum wells Springer Proceedings in Physics, 2001, , 216-217.	0.1	0
191	Antiferromagnetic phase transition in a single MnTe monolayer. Physica E: Low-Dimensional Systems and Nanostructures, 2000, 7, 1006-1010.	1.3	2
192	Exciton dynamics in ZnCdSe/ZnSe ridge quantum wires. Physica E: Low-Dimensional Systems and Nanostructures, 2000, 7, 526-530.	1.3	2
193	High-finesse mid infrared microcavities based on lead salts. Physica E: Low-Dimensional Systems and Nanostructures, 2000, 7, 636-640.	1.3	0
194	6 [micro sign]m vertical cavity surface emitting laser based on IV-VI semiconductor compounds. Electronics Letters, 2000, 36, 322.	0.5	27
195	4.8 μm vertical emitting PbTe quantum-well lasers based on high-finesse EuTe/Pb1â^xEuxTe microcavities. Applied Physics Letters, 2000, 76, 1807-1809.	1.5	50
196	Zeeman mapping of probability densities in square quantum wells using magnetic probes. Physical Review B, 2000, 61, 15617-15620.	1.1	8
197	Single antiferromagnetic MnTe (sub)monolayers in CdTe/CdMgTe quantum wells. Semiconductor Science and Technology, 2000, 15, 506-510.	1.0	7
198	plasma etching of IV-VI semiconductor nanostructures. Semiconductor Science and Technology, 1999, 14, L11-L14.	1.0	25

#	Article	IF	CITATIONS
199	Reflectance difference spectroscopy and magneto-optical analysis of digital magnetic heterostructures. Journal of Vacuum Science & Technology an Official Journal of the American Vacuum Society B, Microelectronics Processing and Phenomena, 1999, 17, 1722.	1.6	1
200	Ultra-high-finesse IV–VI microcavities for the midinfrared. Applied Physics Letters, 1999, 75, 1246-1248.	1.5	33
201	MBE growth of highly efficient lead-salt-based Bragg mirrors on BaF2 (111) for the 4–6î¼m wavelength region. Journal of Crystal Growth, 1999, 201-202, 999-1004.	0.7	6
202	Luminescence of ZnCdSe/ZnSe ridge quantum wires. Applied Physics Letters, 1999, 75, 974-976.	1.5	7
203	High-reflectivity lead-salt-based Bragg mirrors for the mid-infrared range. IEEE Journal of Quantum Electronics, 1999, 35, 1753-1758.	1.0	14
204	Absorption and Photoluminescence Study of Cds Quantum Dots: The Role of Host Matrix and Nanocrystal Size and Density. Materials Research Society Symposia Proceedings, 1999, 571, 69.	0.1	1
205	MnTe fractional monolayers in CdTe/CdMgTe heterostructures: a comparative study of magnetic polarons. Journal of Crystal Growth, 1998, 184-185, 921-925.	0.7	4
206	Photoluminescence and Backscattering Characterization of 6H SiC Implanted with Erbium and Oxygen Ions. Materials Science Forum, 1998, 264-268, 501-504.	0.3	9
207	Lateral confinement in ZnSe/ZnCdSe quantum wells grown on patterned substrates. Applied Physics Letters, 1998, 72, 575-577.	1.5	7
208	Molecular beam epitaxy of ZnCdSe/ZnSe wires on patterned GaAs substrates. Journal of Crystal Growth, 1998, 184-185, 347-351.	0.7	2
209	Direct observation of the LO phonon bottleneck in wide GaAs/AlxGa1â^'xAs quantum wells. Physical Review B, 1997, 55, 5171-5176.	1.1	126
210	Intersubband Dynamics below the Optical Phonon Energy for Single and Coupled Quantum Well Systems. Physica Status Solidi (B): Basic Research, 1997, 204, 208-211.	0.7	2
211	Magneto-Optical Spectroscopy on Digital Magnetic Heterostructures. Physica Status Solidi A, 1997, 164, 331-334.	1.7	2
212	Time resolved studies of intersubband relaxation in GaAs/AlGaAs quantum wells below the optical phonon energy using a free electron laser. Superlattices and Microstructures, 1996, 19, 17-24.	1.4	17
213	Intersubband lifetimes in quantum wells. Solid-State Electronics, 1996, 40, 59-62.	0.8	2
214	Time-Resolved Studies of Intersubband Relaxation Using the free Electron Laser. , 1996, , 31-36.		2
215	Tunable lasers and detectors in the FIR. Infrared Physics and Technology, 1995, 36, 113-122.	1.3	9
216	High repetition rate farâ€infrared pâ€type germanium hot hole lasers. Applied Physics Letters, 1995, 67, 3543-3545.	1.5	14

#	Article	IF	CITATIONS
217	Determination of the intersubband lifetime in Si/SiGe quantum wells. Applied Physics Letters, 1995, 66, 3313-3315.	1.5	17
218	Determination of Landau level lifetimes in AlGaAs/GaAs heterostructures with a ps free electron laser. Applied Physics Letters, 1995, 67, 1110-1112.	1.5	16
219	Turbulence during ergodic divertor experiments in Tore Supra. Nuclear Fusion, 1995, 35, 1357-1367.	1.6	35
220	Influence of impurity absorption on germanium hot-hole laser spectra. Semiconductor Science and Technology, 1994, 9, 638-640.	1.0	18
221	Excite-probe determination of the intersubband lifetime in wide GaAs/AlGaAs quantum wells using a far-infrared free-electron laser. Semiconductor Science and Technology, 1994, 9, 1554-1557.	1.0	47
222	Observation of two emission lines in the p-type-Ge cyclotron resonance laser. IEEE Journal of Quantum Electronics, 1994, 30, 2778-2780.	1.0	0
223	Influence of impurities on broadbandp-type-Ge laser spectra under uniaxial stress. Physical Review B, 1993, 47, 16586-16589.	1.1	2
224	Stimulated emission frompâ€Ge due to transitions between lightâ€hole Landau levels and excited states of shallow impurities. Applied Physics Letters, 1992, 60, 1785-1787.	1.5	16
225	Detailed analysis of the emission spectra of the light-heavy hole p-GE laser. , 1991, , .		0
226	4-6 μm vertical cavity surface emitting lasers based on lead salt compounds. , 0, , .		0
227	Femtosecond dynamics of lead-salt vertical-cavity surface-emitting mid-infrared lasers. , 0, , .		0
228	Comparison of IV-VI semiconductor microcavity lasers for the mid-infrared with active regions of different dimensionality. , 0, , .		1
229	Sub-nanogray detection limit in methylammonium lead triiodide X-ray imaging detectors. , 0, , .		0